Phenomenological description of the two energy scales in underdoped superconducting cuprates

B. Valenzuela and E. Bascones
Instituto de Ciencia de Materiales de Madrid, CSIC. Cantoblanco. E-28049 Madrid, Spain[*]

(Dated: February 5, 2008)

Raman and ARPES experiments have demonstrated that in superconducting underdoped cuprates nodal and antinodal regions are characterized by two energy scales instead of the one expected in BCS. The nodal scale decreases with underdoping while the antinodal one increases. Contrary to the behavior expected for an increasing energy scale, the antinodal Raman intensity decreases with decreasing doping. Using the Yang, Rice and Zhang (YRZ) model, we show that these features are a consequence of the non-conventional nature of the superconducting state in which superconductivity and pseudogap correlations are both present and compete for the phase space.

The pseudogap state of underdoped cuprates is characterized by a nodal-antinodal dichotomy with Fermi arcs at the diagonals of the Brillouin zone (nodal region) and a gapped antinodal region[1,2]. Raman[3,4] and angle resolved photoemission (ARPES) experiments[5] have confirmed that a nodal-antinodal dichotomy is also present in the superconducting state[6]. These results suggest that the superconducting state cannot be simply described by BCS theory, contrary to general believe[7].

Inelastic Raman scattering probes the zero-momentum charge excitations. The response of nodal ($\chi_{B_{2g}}$) and antinodal regions ($\chi_{B_{1g}}$) can be separated. In the superconducting state pair-breaking peaks appear in the spectra. As the normal state of cuprates is characterized by a not yet understood broad continuum, these peaks are better identified in the subtracted response in superconducting and normal states $\Delta\chi_{B_{1g,2g}} = \chi^{SC}_{B_{1g,2g}} - \chi^{N}_{B_{1g,2g}}$. With a standard d-wave BCS gap $\Delta_S \cos(2\phi)$, as generally used for cuprates, the frequency and intensity of these peaks in both B_{2g} and B_{1g} channels would be only controlled by Δ_S.

The experiments[3] reveal that in underdoped cuprates $\Delta\chi_{B_{1g}}$ and $\Delta\chi_{B_{2g}}$ show pair breaking peaks with opposite evolution with doping, instead of the single energy scale. The B_{1g} peak shifts to higher energy and loses intensity with underdoping, while the B_{2g} peak shifts to lower frequency without too much change in intensity. The Raman spectrum, specially the intensity of the B_{1g} peak has been one of the experimental results more difficult to understand. A *modified* BCS gap with higher harmonics[3], and vertex corrections[8] or a very strongly anisotropic renormalization of the quasiparticle[3] have been invoked to explain the B_{1g} peak frequency and intensity, respectively.

ARPES measurements[5] have also uncovered that underdoping leads to an increase in the gap in the antinodal region Δ_{max} and a decrease in the slope of the gap at the nodes, v_Δ, resulting in a U-shape dependence of the gap[5] instead of the V-shape expected from d-wave BCS. In the standard d-wave model, Δ_S gives both v_Δ and Δ_{max}. A single-energy scale and a linear (V-shape) dependence on $\cos(2\phi)$ of the gap are observed in the ARPES and Raman spectrum of overdoped cuprates[2,4].

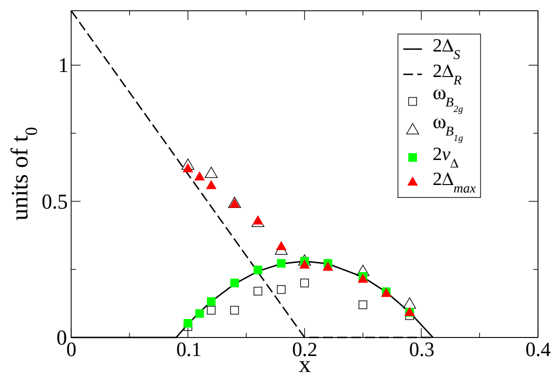

FIG. 1: (Color online) Comparison of pseudogap Δ_R and superconducting Δ_S scales with ARPES nodal v_Δ and antinodal Δ_{max} ones and with the frequency at which B_{1g} ($\omega_{B_{1g}}$) and B_{2g} ($\omega_{B_{2g}}$) Raman responses peak. The parameters used depend on doping as, $\Delta_R(x)/2 = 0.3(1 - x/0.2)$, $\Delta_S(x)/2 = 0.07(1 - 82.6(x - 0.2)^2)$, $t(x) = g_t(x) + 0.169/(1 + x)^2$, $|t'(x)| = g_t(x)|t'_0|$ with $t'_0 = -0.3$, $t''(x) = g_t(x)t''_0$ with $t''_0 = 0.2$. All energies are in units of the bare hopping t_0.

In this letter, we show that the appearance of nodal and antinodal energy scales and the suppression of intensity of $\Delta\chi_{B_{1g}}$ with underdoping are a consequence of the non-conventional nature of the superconducting (SC) state in which superconductivity and pseudogap (PG) correlations are both present and compete for the phase space and not just a modified BCS gap. We assume that the PG strength, given by Δ_R vanishes at a topological quantum critical point (QCP), and that the SC order parameter Δ_S follows the critical temperature. Fig. 1 and the evolution of the Raman intensity with doping x are our main results. Only the nodal energy scales follow the non-monotonic dependence of the SC order parameter, being the slope of the gap at the nodes v_Δ a good measure of Δ_S. The antinodal energy scale, i.e. the location of the B_{1g} Raman peak $\omega_{B_{1g}}$ and the maximum gap Δ_{max} in ARPES, is intimately connected with the PG. The Raman spectra is calculated at the bubble level. The decrease of intensity in the B_{1g} channel with underdoping is not due to vertex corrections, but to the competition of PG and superconductivity in the antinodal

region. The renormalization of the quasiparticle weight g_t just enhances this effect.

We use the ansatz proposed by Yang, Rice and Zhang[9] (YRZ) for the PG. The YRZ model assumes that the PG can be described as a doped spin liquid and proposes a phenomenological Green's function to characterize it.

$$G^{YRZ}(\mathbf{k},\omega) = \frac{g_t}{\omega - \xi_{\mathbf{k}} - \Sigma_R(\mathbf{k},\omega)} + G_{inc}. \qquad (1)$$

Here $\xi_{\mathbf{k}} = \epsilon_{0\mathbf{k}} - 4t'(x)\cos k_x \cos k_y - 2t''(x)(\cos 2k_x + cos2k_y) - \mu_p$, $\epsilon_{0\mathbf{k}} = -2t(x)(\cos k_x + \cos k_y)$ and μ_p is determined from the Luttinger sum rule. $\Sigma_R(\mathbf{k},\omega) = \Delta_R(\mathbf{k})^2/(\omega + \epsilon_{0\mathbf{k}})$ diverges at zero frequency at the umklapp surface $\epsilon_{0\mathbf{k}}$, and $\Delta_R(\mathbf{k}) = \Delta_R(x)/2(\cos k_x - \cos k_y)$. The coherent part is similar to the BCS diagonal Green's function with the non-trivial difference that in BCS, the self-energy diverges at the Fermi surface (FS) and not at the umklapp one. Besides there is no off-diagonal component of the Green's function in our case and Δ_R does not break any symmetry. For finite Δ_R the quasiparticle peak is split into two and the FS consists of hole pockets close to $(\pm\pi/2, \pm\pi/2)$. At x_c, $\Delta_R(x)$ vanishes at a topological transition and a complete FS is recovered. Following predictions of mean field theory[10] the coherent spectral weight factor, $g_t = 2x/(1+x)$, decreases with underdoping and vanishes at half filling. We use the same parameters proposed in the original paper[9], see Fig. 1.

Superconductivity is introduced in the standard way[11] as in Ref.[9]. The diagonal Green's function becomes

$$G^{RVB}_{SC}(\mathbf{k},\omega) = \frac{g_t}{\omega - \xi_{\mathbf{k}} - \Sigma_R(\mathbf{k},\omega) - \Sigma_S(\mathbf{k},\omega)}. \qquad (2)$$

$\Sigma_S(\mathbf{k},\omega) = |\Delta_S^2(\mathbf{k})|/(\omega + \xi(\mathbf{k}) + \Sigma_R(\mathbf{k},-\omega))$ is the SC self energy with $\Delta_S(\mathbf{k}) = \Delta_S(x)/2(\cos k_x - \cos k_y)$ with doping dependence given in Fig. 1. Each quasiparticle peak splits into four with energies $\pm E_\pm$.

$$\begin{aligned}(E^{\pm}_{\mathbf{k}})^2 &= \Delta^2_{R\mathbf{k}} + \frac{\xi^2_{\mathbf{k}} + \xi^2_{0\mathbf{k}} + \Delta^2_{S\mathbf{k}}}{2} \pm (E^{SC}_{\mathbf{k}})^2 \\ (E^{SC}_{\mathbf{k}})^2 &= \sqrt{(\xi^2_{\mathbf{k}} - \xi^2_{0\mathbf{k}} + \Delta^2_{S\mathbf{k}})^2 + 4\Delta^2_{R\mathbf{k}}((\xi_{\mathbf{k}} - \xi_{0\mathbf{k}})^2 + \Delta^2_{S\mathbf{k}})}\end{aligned}$$

The spectral functions $A(\mathbf{k},\omega) = -2\mathrm{Im}G(\mathbf{k},\omega)$ and $B(\mathbf{k},\omega) = -2\mathrm{Im}F(\mathbf{k},\omega)$ with $F(\mathbf{k},\omega)$ the anomalous Green's function are

$$\begin{aligned}A(\mathbf{k},\omega) &= g_t\pi\{(v^-_{\mathbf{k}})^2\delta(\omega + E^-_{\mathbf{k}}) + (u^-_{\mathbf{k}})^2\delta(\omega - E^-_{\mathbf{k}}) \\ &\quad + (v^+_{\mathbf{k}})^2\delta(\omega + E^+_{\mathbf{k}}) + (u^+_{\mathbf{k}})^2\delta(\omega - E^+_{\mathbf{k}})\}, \\ B(\mathbf{k},\omega) &= g_t\pi\{u^-_{\mathbf{k}}v^-_{\mathbf{k}}(\delta(\omega + E^-_{\mathbf{k}}) + \delta(\omega - E^-_{\mathbf{k}})) \\ &\quad + u^+_{\mathbf{k}}v^+_{\mathbf{k}}(\delta(\omega + E^+_{\mathbf{k}}) + \delta(\omega - E^+_{\mathbf{k}}))\}, \qquad (3)\end{aligned}$$

with coherence factors $v^{2\pm}_{\mathbf{k}} = \frac{1}{2}\left(a^{\pm}_{\mathbf{k}} - b^{\pm}_{\mathbf{k}}/E^{\pm}_{\mathbf{k}}\right)$ and $u^{2\pm}_{\mathbf{k}} = \frac{1}{2}\left(a^{\pm}_{\mathbf{k}} + b^{\pm}_{\mathbf{k}}/E^{\pm}_{\mathbf{k}}\right)$, where $a^{\pm}_{\mathbf{k}} = \frac{1}{2}(1 \pm (\xi^2_{\mathbf{k}} - \xi^2_{\mathbf{k0}} + \Delta^2_{S\mathbf{k}})/E^{SC}_{\mathbf{k}})$ and $b^{\pm}_{\mathbf{k}} = \xi_{\mathbf{k}}a^{\pm}_{\mathbf{k}} \pm \Delta^2_{R\mathbf{k}}(\xi_{\mathbf{k}} - \xi_{\mathbf{k0}})$.

In the bubble approximation[12] the Raman response is

$$\begin{aligned}\mathrm{Im}\{\chi_{\gamma_\nu}(\Omega)\} &= \sum_{\mathbf{k}}(\gamma^{\nu}_{\mathbf{k}})^2 \int \frac{d\omega}{4\pi}(n_F(\omega) - n_F(\omega + \Omega)) \\ &\quad \{A(\mathbf{k},\omega+\Omega)A(\mathbf{k},\omega) - B(\mathbf{k},\omega+\Omega)B(\mathbf{k},\omega)\}. \qquad (4)\end{aligned}$$

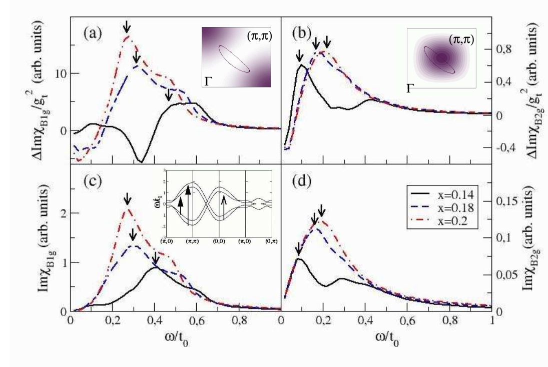

FIG. 2: Insets in (a) and (b): Raman vertices $(\gamma^{B_{1g}}_{\mathbf{k}})^2$ and $(\gamma^{B_{2g}}_{\mathbf{k}})^2$ in the first quadrant of the Brillouin zone (BZ), with the Fermi pocket for $x = 0.14$ drawn. Inset in (c): bands for $x = 0.14$ in the SC state. The arrows signal the possible optical transitions. Main figures (a) and (b) subtracted Raman response in B_{1g} and B_{2g} polarizations divided by the coherent weight factor g_t^2, for $x = 0.14$ and $x = 0.18$ in the underdoped regime and to $x_c = 0.20$. (c) and (d) full Raman response in the B_{1g} and B_{2g} channels respectively for the same dopings. Raman units are the same for all dopings. The arrows indicate the position, $\omega_{B_{1g}}$ and $\omega_{B_{2g}}$, and intensity of the pair breaking peaks. The δ functions in Eq. 3 have been replaced by Lorenzians with a width of $0.05t(x)$ with $t(x)$ given in Fig. 2a.

Here $n_F(\omega)$ is the Fermi function, $\nu = B_{1g}, B_{2g}$ and $\gamma^{\nu}_{\mathbf{k}}$, the B_{1g} and B_{2g} Raman vertices, are proportional to $\cos k_x - \cos k_y$ and $\sin k_x \sin k_y$ respectively.

The dependence on x of the nodal and antinodal subtracted Raman spectra $\Delta\chi$ can be seen in Fig. 2a and 2b. Two different energy scales $\omega_{B_{1g}}$ and $\omega_{B_{2g}}$ appear for finite Δ_R. These scales, signalled by an arrow in Fig. 2, are plotted in Fig. 1. At $x_c = 0.2$ the PG vanishes and $\Delta\chi_{B_{1g}}$ and $\Delta\chi_{B_{2g}}$ peaks appear at an energy close to $2\Delta_S$. This is the expected behavior for a BCS superconductor[13]. On the contrary, as x is reduced the $\Delta\chi_{B_{1g}}$ peak shifts to larger frequency and its intensity decreases, while the $\Delta\chi_{B_{2g}}$ peak shifts to lower frequency with a weakly x-dependent intensity. This behavior resembles very much the experimental one[3]. In Fig. 2a and 2b the spectra have been divided by g_t^2 to emphasize that the suppression of the intensity in the B_{1g} channel with underdoping is not only due to the reduction of the coherent part, as proposed in[3]. With g_t^2 included the weakening of the B_{1g} transition with underdoping is enhanced and the B_{2g} signal decreases.

The appearance of two different energy scales for B_{1g} and B_{2g} response is associated to the two pair-breaking transitions in the inset of Fig. 2c with energies $2E_\pm(\mathbf{k})$. The distinction between nodal and antinodal signal has its origin in the coherence factors $u^2_\pm(\mathbf{k})v^2_\pm(\mathbf{k})$ which weight each transition. Shown in Fig. 3a (Fig. 3b) for $x = 0.14$, $u^2_-(\mathbf{k})v^2_-(\mathbf{k})$ $(u^2_+(\mathbf{k})v^2_+(\mathbf{k}))$, weights more heavily the nodal (antinodal) region. The B_{2g} and B_{1g} spectra are respectively dominated by the transitions with

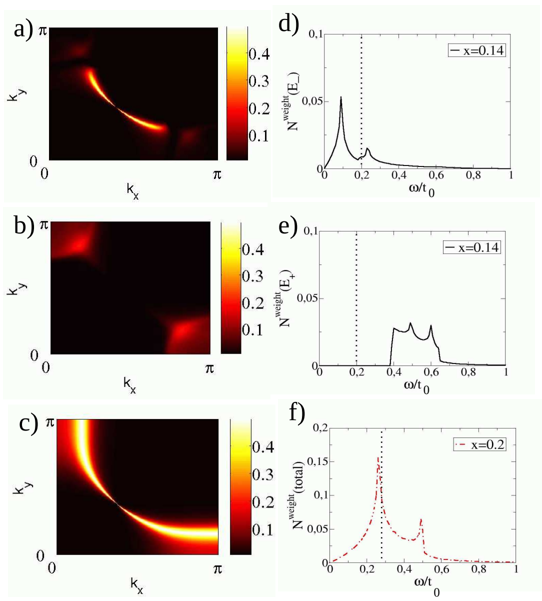

FIG. 3: (a) to (c) coherence factors, in the first quadrant of the BZ, corresponding to the pair breaking transitions with energies $2E_\pm$ (see text). The weighted densities of transitions $N^{weight}(E_\pm)$ are plotted in (d) to (f). $2\Delta_S$ is marked with a dotted line. The added coherence factors and total weighted density of transitions for $x_c = 0.2$ (critical doping) are shown in (c) and (e) recovering the d-wave BCS result.

energy $2E_-$ and $2E_+$. The maxima in the Raman spectra in Fig. 2a and 2b arise from the peaks in the densities of transitions $N^{weight}_{2E_\pm} = \sum_{\mathbf{k}} u^2_\pm(\mathbf{k}) v^2_\pm(\mathbf{k}) \delta(\omega - 2E_\pm(\mathbf{k}))$. In Fig. 3d $N^{weight}_{2E_-}$ peaks at a frequency smaller than $2\Delta_S$. $\omega_{B_{2g}}$ depends not only on Δ_S but also on the length of the Fermi pockets along $(\pi,0)$-$(0,\pi)$ as its value comes from the edges of the Fermi pockets. Due to the shrinking of the pockets with increasing Δ_R, $\omega_{B_{2g}}$ is shifted to lower frequencies with underdoping, even if a doping independent Δ_S is used. In Fig. 3e, the energy at which $N^{weight}_{2E_+}$ peaks is determined by a saddle-point close to $(\pi,0)$, along $(\pi,0)-(\pi,\pi)$ and is bigger than $2\Delta_S$. In the UD region, this energy is mainly controlled by Δ_R. If $x \geq x_c$, only one of the pair-breaking transitions gives a finite contribution for a given $\mathbf{k}$. A complete d-wave superconducting gap is recovered and, as shown in Fig. 3c it is tracked by the added coherence factors $u^2_+(\mathbf{k})v^2_+(\mathbf{k}) + u^2_-(\mathbf{k})v^2_-(\mathbf{k})$. The maximum in $N^{weight}_{E_-}$ is not anymore a maximum of the total density $N^{weight}_{tot} = N^{weight}_{E_-} + N^{weight}_{E_+}$, plotted in Fig. 3f, but both densities of transitions match perfectly. N^{weight}_{tot} is now the meaningful quantity. It peaks close to $2\Delta_S$ recovering the BCS single-energy behavior[13].

A third *crossing* transition, with energy $E_-(\mathbf{k}) + E_+(\mathbf{k})$, and larger intensity in the B_{1g} channel is also allowed if Δ_R is finite, as shown in the inset of Fig. 2c. Its effect is small in $\Delta\chi$, as it is expected in both the PG and the SC state. The total responses $\chi^{SC}_{B_{1g}}$ and $\chi^{SC}_{B_{2g}}$ including the contribution of this crossing transition in the SC state are plotted in Figs. 3c and 3d. It is not easy to distinguish this transition from the pair-breaking ones. To the best of our knowledge this transition has not been found yet in the PG state but it could be hidden in the broad background due to strong inelastic scattering.

As expected for a gap with nodes, the B_{2g} response in Fig. 3d is linear at low frequencies. The slope is doping independent. This independence, observed also experimentally[3], comes from a cancellation between the dependencies of the quasiparticle weight squared g_t^2, the SC order parameter, Δ_S, and the density of states, via the renormalization of the band parameters.

The nodal and antinodal scales can be also seen in ARPES. As discussed in ref.[9] for $x < x_c$ in the PG state, the FS consists of closed hole pockets. However, due to the weak spectral weight of the quasiparticle pole in the outer edge of the pocket, the ARPES spectra resembles the Fermi arcs observed experimentally. The length of these arcs increases with doping, as seen in Fig. 4a and Fig. 4b. A complete FS is recovered when $\Delta_R = 0$ in Fig. 4c. In the absence of a complete FS, to analyze the $\mathbf{k}$-dependence of the gap we take the surface with maximal intensity $\omega = 0$ and $\Delta_S = 0$. This surface, signalled in blue in the pictures, resembles the one interpreted experimentally as the underlying FS. To compare with experiments[5] we define v_Δ as the derivative of the energy with respect to $\cos k_x - \cos k_y$ at the nodes[14] and Δ_{max} as the maximum gap along this surface. Shown in Fig. 4d for $x = 0.05$, when Δ_S is zero but Δ_R finite, the energy vanishes along the arc and a gap opens linearly with $\cos k_x - \cos k_y$ from the arc edge. Δ_{max} increases with underdoping. A finite Δ_S opens a gap along the arc in Fig. 4e. This gap depends linearly on $\cos k_x - \cos k_y$, with slope v_Δ very close to Δ_S. Outside the arc[15], the gap depends on both Δ_R and Δ_S. In this UD SC region v_Δ increases with doping and Δ_{max} decreases (see Fig. 1). Correspondingly, the spectra does not depend linearly on $\cos k_x - \cos k_y$ but has a U-shape dependence on $\cos k_x - \cos k_y$ with a kink around the arc edge. Deviations from linearity increase with underdoping. In Fig. 4f, at $x = x_c$, the linear V-shape BCS dependence re-appears and v_Δ and Δ_{max} converge.

The evolution of ARPES scales v_Δ and Δ_{max}, with doping is plotted in Fig. 1, and compared with the ones found in Raman and the input Δ_S and Δ_R. The similarity with experimental data is striking[3]. With the $\Delta_S(x)$ used, $\omega_{B_{2g}}$ and v_Δ are non-monotonic on doping. On the other hand, the frequency at which B_{1g} peaks $\omega_{B_{1g}}$ follows very closely $2\Delta_{max}$ and both decrease as Δ_R does. Twice the gap value at $(\pi,0)$, sometimes compared in the literature with $\omega_{B_{1g}}$, is expected to be a bit larger than $2\Delta_{max}$ plotted here. The nodal and antinodal scales merge when the pseudogap correlations disappear.

In conclusion, we have reproduced the deviations from BCS in Raman and ARPES experiments in underdoped superconducting cuprates. Nodal and antinodal energy scales with opposite doping dependence appear in both

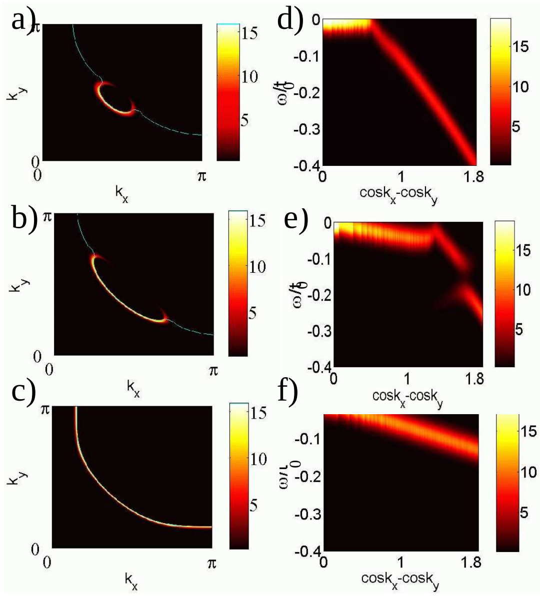

FIG. 4: (a) to (c) Map of ARPES intensity in the first quadrant of the BZ, at zero frequency and zero Δ_S for (a) $x = 0.05$, (b) $x = 0.14$ and (c) $x_c = 0.20$. In blue, the maximum intensity surface. (d) to (f) Energy spectrum corresponding to (d) x=0.05, (e) x=0.14 and (f) x=0.20, along the surface marked in (a) to (c). Δ_S is finite in (e) and (f). The δ functions in $A(\mathbf{k}, \omega)$, have been replaced by lorenzians of width $0.001t_0$ and the spectral function convoluted with a gaussian of width $0.02t_0$ ($\sim 6-10meV$) and a temperature $T = 0.001t_0$.

spectra. The nodal B_{2g} response, peaks at a frequency $\omega_{B_{2g}}$ which qualitatively follows the doping dependence of the superconducting order parameter Δ_S. On the contrary, the energy of the pair breaking transitions in the antinodal region, $\omega_{B_{1g}}$, decreases monotonically with increasing doping and its intensity decreases with underdoping due to the competition between pseudogap and superconducting correlations. Twice the maximum value of the ARPES gap Δ_{max} along the maximum intensity surface follows very closely $\omega_{B_{1g}}$. Within this model the slope of the gap at the nodes, v_Δ, as measured by ARPES, is a good measure of Δ_S while the maximum value of the gap Δ_{max} arises from an interplay between the pseudogap Δ_R and Δ_S. We emphasize that we have not tried to fit the experiments but just taken the values proposed in the YRZ paper[9]. For the values used, x_c and optimal doping coincide. If this is not the case[16], it is x_c which controls the emergence of anomalous behavior.

Similar two-scale behavior could appear in other models with a QCP[17]. Possible differences could be the decreasing spectral weight with underdoping, important for the constancy of the slope in B_{2g} channel. which a priori is not expected in other QCP models. In the YRZ ansatz the FS is truncated without breaking of symmetry and a topological transition happens at x_c, in agreement with experiments[16] and Dynamical Mean Field Theory[18]. Our results suggest that the pseudogap is not a precursor to the superconductivity but has a different origin and persists in the superconducting state and that the antinodal scale depends on both the pseudogap and the superconducting order parameter. The smooth convergence of the antinodal scale with the superconducting order parameter and a peak in $\Delta\chi_{B_{1g}}$ are hard to understand in models with separation in $\mathbf{k}$-space in which antinodal quasiparticles, responsible of the pseudogap, do not participate in superconductivity[19]. While not included here, we believe that the appearance of two energy scales in the SC state is robust enough to survive inelastic scattering.

Acknowledgments

We thank M. Le Tacon, A. Sacuto, L. Tassini, R. Hackl, J. Carbotte and G. Kotliar for discussions and M.A.H Vozmediano, A.V. Chubukov, F. Guinea and T.M. Rice for discussions and reading of the preprint. Funding from MCyT through MAT2002-0495-C02-01, FIS2005-05478-C02-01 and Ramon y Cajal and from Consejería de Educación de la Comunidad de Madrid and CSIC through 200550M136 and I3P is acknowledged.

* Electronic address: leni@icmm.csic.es, belenv@icmm.csic.es

[1] T. Timusk and B. W. Statt, Rep. Prog. Phys. **62**, 61 (1999); M. R. Norman, D. Pines, and C. Kallin, Adv. Phys. **54**, 715 (2005).

[2] A. Damascelli, Z. Hussain, and Z-X. Shen, Rev. Mod. Phys. **75**, 473 (2003).

[3] M. Le Tacon *et al*, Nature Physics **2**, 537 (2006).

[4] T. P. Devereaux, and R. Hackl, Rev. Mod. Phys. in press.

[5] J. Mesot *et al* Phys. Rev. Lett. **83**, 840 (1999). S. V. Borisenko, *et al* Phys. Rev. B **66**, 140509 (2002). Tanaka *et al* Science **314**, 1910 (2006). Kondo *et al* cond-mat/0611517.

[6] C. Panagopoulos and T. Xiang, Phys. Rev. Lett. **81**, 2336 (1998).

[7] J. Zaanen, et al., Nature Physics **2**, 138 (2006).

[8] R. Zeyher and A. Greco, Phys. Rev. Lett. **89**, 177004 (2002); Y. Gallais *et al*, Phys. Rev. B **71**, 012506 (2005); A.V. Chubukov, T.P. Devereaux and M.V. Klein, Phys. Rev. B **73**, 094512 (2006).

[9] K-Y. Yang, T. M. Rice, and F-C Zhang, Phys. Rev. B **73**, 174501 (2006).

[10] F. C. Zhang, C. Gros, T. M. Rice, and H. Shiba, Supercond. Sci. Techmol. **1**, 36-46 (1988).

[11] A. A. Abrikosov, L. P. Gor'kov, and I. E. Dzyaloshinaskii, *Methods of Quantum Field Theory in Statistical Physics*, (R.A. Silverman, revised edn. Dover, New York,(1975)).

[12] G. Mahan, *Many Particle Physics*, (Plenum Press, New York and London, 1990).

[13] In the continuum the peak in $\Delta\chi_{B_{1g}}$ is at $2\Delta_S$. In a lattice two peaks appear, the one at higher energy is due to band structure effects and ignored in the discussion.

[14] v_Δ is normalized to Δ_{max} for $\Delta(\phi) = \Delta_{max} cos(2\phi)^5$.

[15] The suppression of the intensity for some **k** in the SC state is due to the mixing between the $\pm E_\pm$ bands.

[16] J. L. Tallon, and J. W. Loram, Physica C **349**, 53 (2001).

[17] S. Chakravarty, R. B. Laughlin, D. K. Morr, and C. Nayak, Phys. Rev. B **63**, 094503 (2001); C. M. Varma, Phys. Rev. Lett **83**, 3538 (1999); L. Benfatto, S. Caprara, C. Di Castro, Eur. Phys. J. B **71**, 95 (2000).

[18] T. D. Stanescu and G. Kotliar, Phys. Rev. B **74**, 125110 (2006).

[19] D. Pines, cond-mat/0404151 (preprint).